PHYSICAL REVIEW E VOLUME 61, NUMBER 5 MAY 2000

Noncollinear generation of optical spatiotemporal solitons and application to ultrafast digital logic

Xiang Liu, Kale Beckwitt, and Frank Wise
Department of Applied Physics, Cornell University, Ithaca, New York 14853
(Received 9 December 1999)

We demonstrate theoretically and experimentally that spatiotemporal solitons can be generated through noncollinear second-harmonic generation. The resulting *Y* geometry could be used to implement an optical AND gate with ultrafast, high-contrast operation but without sensitivity to the phases of the input pulses.

PACS number(s): 42.65.Tg, 42.79.Ta

Optical solitons are localized electromagnetic waves that propagate stably in nonlinear media despite the presence of group-velocity dispersion (GVD) and/or diffraction. Spatiotemporal solitons (STS) result from the simultaneous balance of diffraction and dispersion by self-focussing and nonlinear phase-modulation, respectively. STS were recently generated experimentally, in quadratic media [1]. Liu *et al.* reported the formation of pulses that overcome diffraction in one transverse spatial dimension as well as group-velocity dispersion to reach stable or periodically stable beam size and pulse duration; diffraction occurs in the remaining transverse spatial dimension. These pulses are referred to as two-dimensional (2D) STS, to distinguish them from 3D STS, which are localized in all three dimensions [2]. In quadratic media, the soliton actually consists of at least two fields at different frequencies, coupled and mutually trapped by the nonlinear interaction.

In addition to the scientific interest in STS, such pulses could be the basis of ultrafast optical digital logic in the future [3]. Fast, highly parallel switching is possible based on interactions of STS. Quadratic solitons can be expected to require lower powers than solitons in Kerr media, if the latter can be formed at all; Kerr solitons are theoretically unstable in more than one transverse dimension in the absence of some saturation or loss. Switching based on head-on collisions of stationary spatial solitons in slab waveguides [4] and bulk quadratic crystals [5] was recently reported. For ultrafast photonic processing, the temporal profiles of the interacting optical beams should naturally be confined. Experimental realization of two-dimensional soliton processing should be easier than in three dimensions, and the slab waveguide geometry potentially allows for tailoring the dispersion characteristics to those needed for STS. Macleod *et al.* [3] point out that these benefits may offset the loss of one dimension of spatial parallelism, and motivate studies of 2D STS.

In this Rapid Communication we describe the generation of 2D STS in a different geometry. Degenerate, noncollinear beams of short pulses are arranged for phase-mismatched second-harmonic generation (SHG). Through nonlinear trapping of the original fundamental fields, femtosecond-duration STS that propagate along the bisector of the angle between input beams are formed. This *Y* geometry for STS generation (Fig. 1) naturally lends itself to all-optical logic operations. In contrast to devices based on soliton collisions, this approach has the benefit of being insensitive to the phases of the input pulses.

The noncollinear production of STS was inspired by a proposal for STS-based optical logic from Drummond, Kheruntsyan, and He [6]. In the interest of exploiting a phase-insensitive interaction, these workers proposed the formation of STS from input signals with orthogonal polarizations. This implies a type-II interaction, with the attendant group-velocity mismatch (GVM) between input beams. GVM between the fundamental and harmonic fields places significant constraints on the conditions under which STS will form. With large GVM, the harmonic field will tend to propagate away from the fundamental, which degrades the mutual trapping required for STS formation. We have shown that the effects of GVM between fundamental and harmonic pulses can be partially overcome by employing the cascade process at large phase mismatch [1,7], and it is known that quadratic solitons can form despite the presence of this GVM [8]. GVM between input fundamental pulses further complicates the process; in that case all three waves have different velocities, so it is not clear that mutual trapping is possible. To avoid this difficulty, we considered only type-I interactions.

We are interested in the situation where fundamental fields E_L and E_R cross near the entrance face of a quadratic medium. The equations that govern the evolution of the field components (assumed constant in the *x* direction) are

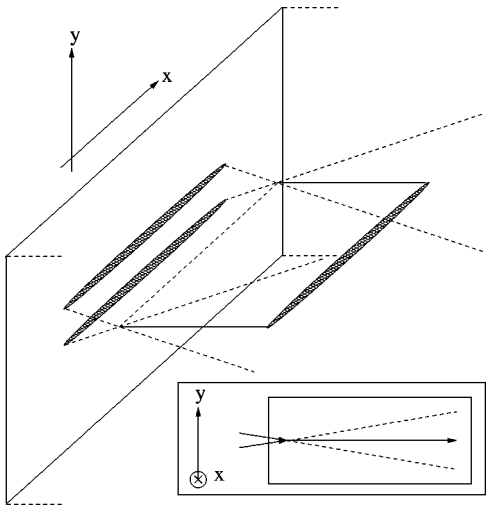

FIG. 1. Schematic geometry for noncollinear STS generation.

$$\left(\frac{\partial}{\partial z}+\frac{iL_{NL}}{4L_{DS1}}\frac{\partial^2}{\partial t^2}+\frac{iL_{NL}}{4L_{DF1}}\frac{\partial^2}{\partial y^2}+\frac{L_{NL}}{L_{wL}}\frac{\partial}{\partial y}\right)E_L = iE_R^* E_{Msh}e^{i\Delta k_M z}+iE_L^* E_{Lsh}e^{i\Delta k_L z},$$

$$\left(\frac{\partial}{\partial z}+\frac{iL_{NL}}{4L_{DS1}}\frac{\partial^2}{\partial t^2}+\frac{iL_{NL}}{4L_{DF1}}\frac{\partial^2}{\partial y^2}+\frac{L_{NL}}{L_{wR}}\frac{\partial}{\partial y}\right)E_R = iE_L^* E_{Msh}e^{i\Delta k_M z}+iE_R^* E_{Rsh}e^{i\Delta k_R z},$$

$$\left(\frac{\partial}{\partial z}+\frac{iL_{NL}}{4L_{DS2}}\frac{\partial^2}{\partial t^2}+\frac{iL_{NL}}{4L_{DF2}}\frac{\partial^2}{\partial y^2}+\frac{L_{NL}}{L_{GVM}}\frac{\partial}{\partial t}\right)E_{Msh} = 2iE_L E_R e^{-i\Delta k_M z}, \quad (1)$$

$$\left(\frac{\partial}{\partial z}+\frac{iL_{NL}}{4L_{DS2}}\frac{\partial^2}{\partial t^2}+\frac{iL_{NL}}{4L_{DF2}}\frac{\partial^2}{\partial y^2}+\frac{L_{NL}}{L_{WL}}\frac{\partial}{\partial y}+\frac{L_{NL}}{L_{GVM}}\frac{\partial}{\partial t}\right)E_{Lsh} = iE_L E_L e^{-i\Delta k_L z},$$

$$\left(\frac{\partial}{\partial z}+\frac{iL_{NL}}{4L_{DS2}}\frac{\partial^2}{\partial t^2}+\frac{iL_{NL}}{4L_{DF2}}\frac{\partial^2}{\partial y^2}+\frac{L_{NL}}{L_{WR}}\frac{\partial}{\partial y}+\frac{L_{NL}}{L_{GVM}}\frac{\partial}{\partial t}\right)E_{Rsh} = iE_R E_R e^{-i\Delta k_R z}.$$

E_{Msh}, E_{Lsh}, and E_{Rsh} are the fields at the sum frequency of E_L and E_R, second-harmonic of E_L, and second-harmonic of E_R, respectively. The propagation distance z is in units of the nonlinear length $L_{\mathrm{NL}}=n\lambda/(\pi\chi^{(2)}E_0)$, with E_0 related to the peak intensity of an input pulse by $I_0=(\varepsilon/\mu)^{1/2}|E_0|^2/2$. The transverse spatial coordinate y is in units of the beam waist ω_0. $L_{\mathrm{DS1(2)}}$ and $L_{\mathrm{DF1(2)}}$ are the dispersion and diffraction lengths of the fundamental (harmonic) waves. L_{WL} (L_{WR}) is the walk-off length for the left (right) input E_L (E_R). L_{GVM} is the distance over which the harmonic pulse would move one pulse duration away from the fundamental pulse in time if the propagation were linear. The wave-vector mismatches are $\Delta k_M=k_{\mathrm{MSH}}-k_L-k_R$, $\Delta k_L=k_{Lsh}-2k_L$, and $\Delta k_R=k_{Rsh}-2k_R$. The generated 2D STS will be confined in time and the y direction. We neglect the effect of the Kerr nonlinearity (n_2) since it contributes $<10\%$ of the overall nonlinear phase shift under our experimental conditions.

The equations are solved with a symmetric split-step beam-propagation method. The propagation step along the z axis is fine enough to ensure total energy conservation to within 1%. With an input consisting of only E_L (E_R) and appropriate choices for intensity and phase mismatch, the input pulse evolves to an STS, as shown in Figs. 2(a) and 2(b). The temporal shape of the pulse is stationary, so only the time-integrated intensity of the fundamental field along the y axis is plotted. The individual STS have a beam diameter of 58 μm, and they propagate toward points $\sim$400 μm apart on the exit face of the crystal. With both E_L and E_R present as inputs, the pulses merge and evolve to a STS that propagates between the input-beam directions [Fig. 2(c)]. A physical picture of this process is that the two input fields exert an attractive force on each other via the middle harmonic field to which they are both coupled. Two effects come into play: the harmonic field attracts the input fundamental fields, and more importantly, the nonlinear phase shift acquired by the total fundamental field causes some self-focusing of the input beams. Since the attraction arises from the beam-coupling terms in the first three equations in (1), the force is not sensitive to the initial phases of the input fundamental fields; the sum-frequency field can always adjust its phase to achieve a certain phase mismatch. We are not considering soliton fusion here; the pulses that merge to form the STS are themselves *not* STS when they merge, so the lack of phase-sensitivity is not so surprising. The intensity of the STS exhibits periodic oscillation, as expected for quadratic solitons [9].

A more detailed characterization of the calculated STS is presented in Fig. 3. The spatiotemporal profile of the STS at the exit face of the SHG crystal is shown in Fig. 3(a), while Fig. 3(b) shows the time-integrated intensity profile across the y axis. The spatiotemporal profile is symmetric as expected [10], and the beam is $\sim$40% narrower than the input beams. The wings on the pulse [which are visible in Fig. 2(c)] arise from the mismatch between the STS solution and the launched fields. Finally, the temporal profile of the STS at the central y position ($y=0$) is shown in Fig. 3(c). The

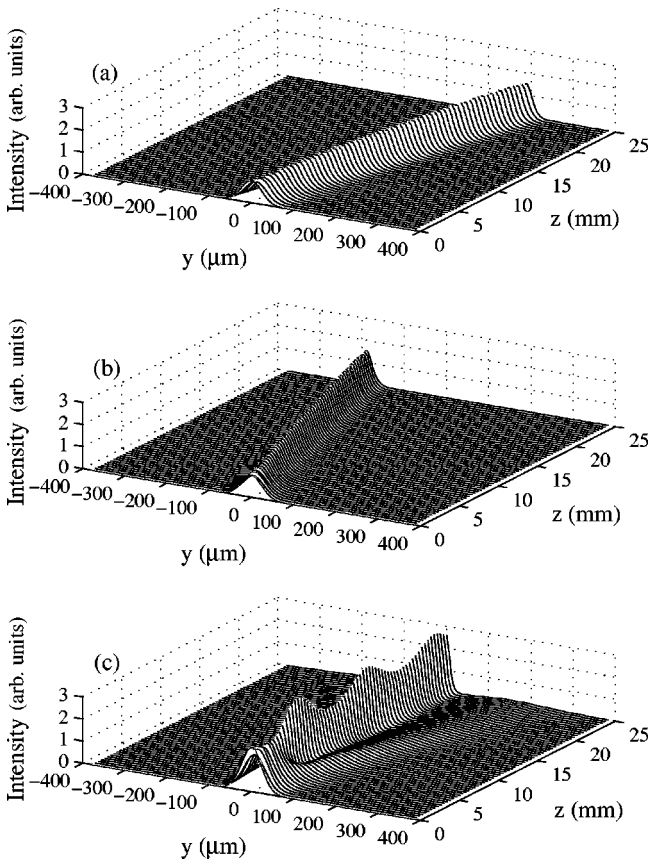

FIG. 2. Calculated STS propagation under different input conditions. (a) Left input field E_L only, (b) Right input field E_R only, and (c) E_L and E_R together. Simulation parameters: $I=6.5$ GW/cm^2, $L_{\mathrm{NL}}=0.55$ mm, total propagation length $L=25$ mm, $\Delta k_M L=-60\pi$, $\Delta k_L L=\Delta k_R L=-65\pi$. $L_{\mathrm{DS1}}=4.5$ mm, $L_{\mathrm{DS2}}=11$ mm, $L_{\mathrm{DF1}}=5$ mm, $L_{\mathrm{DF2}}=10$ mm, $L_{\mathrm{GVM}}=1.4$ mm, and $L_{\mathrm{wL}}=-L_{\mathrm{wR}}=6$ mm. The temporal shape of the pulse is stationary, so only the time-integrated intensity of the fundamental field along the y axis is plotted.

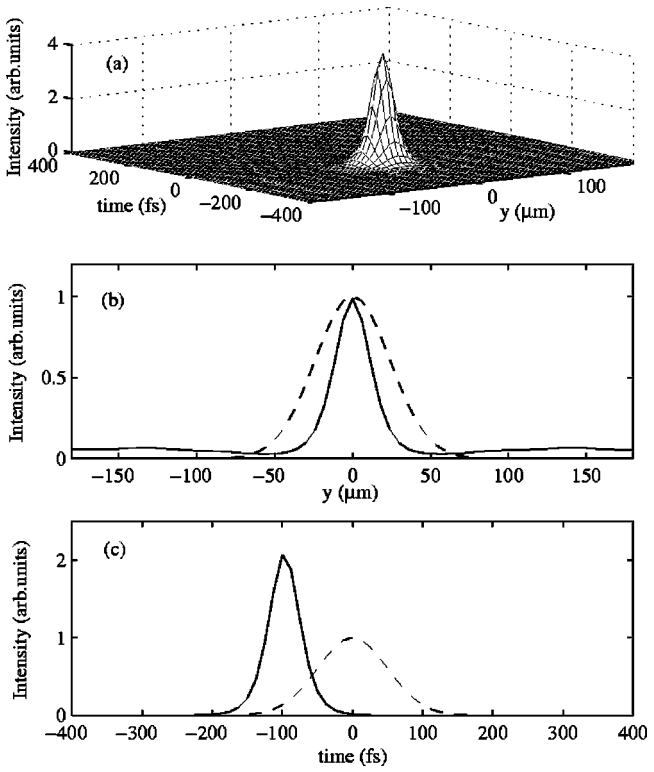

FIG. 3. Calculated spatiotemporal profile of the STS at the exit face of the crystal with two input fields [corresponding to case (c) in Fig. 2]: (a) 3D plot, (b) time-integrated spatial profile of the STS along the y axis, and (c) temporal profile at the central y position. The dashed lines are the profiles of the input pulses.

harmonic field (not shown) is found to be mutually trapped with the fundamental. GVM causes a weak initial radiation of energy; $>98\%$ of the total energy is converted to the STS.

The primary obstacle to the experimental realization of STS in short propagation distances is the the required large and anomalous GVD. Tilting of the pulse wave fronts can be used to simultaneously provide such GVD and reduce or even nullify the GVM [11]. This technique was employed in the generation of temporal [12] and spatiotemporal [1] solitons in quadratic media.

The experimental setup is similar to that described in [1]. Pulses of duration 120 fs and energy up to 1 mJ at wavelength 808 nm are produced by a Ti:sapphire regenerative amplifier. The quadratic nonlinear medium is a 25-mm long Ba_2BO_4 (BBO) crystal cut for type-I SHG. The phase mismatches are set to $\Delta k_M L = -60\pi$ and $\Delta k_L L \sim \Delta k_R L \sim -65\pi$ ($\Delta k < 0$ corresponds to a self-focusing effective nonlinearity). A diffraction grating tilts the pulse wave front in the x-z plane. The effective $L_{\mathrm{GVM}} = 1.4$ mm, and the dispersion lengths are $L_{\mathrm{DS1}} = 4.5$ mm and $L_{\mathrm{DS2}} = 11$ mm. The beam passes through a metal mask to produce two equally intense circular beams propagating parallel to each other. A 200-mm cylindrical lens (focusing along the y axis) produces elliptical spots with dimensions of 58 μm and 3.2 mm in the y and x directions, respectively (Fig. 1). The corresponding lengths for diffraction in the y direction are $L_{\mathrm{DF1}} \sim 5$ mm and $L_{\mathrm{DF2}} \sim 10$ mm. After focusing and inside the crystal, the angle between the beams is $\sim 0.6°$. Each input beam evolves to a STS when the other beam is blocked. The threshold for STS formation is ~ 7.5 GW/cm^2, and experimental STS generated at this intensity are shown in Figs. 4(a) and 4(b). The left column of Fig. 4(a) shows the image of the beam at the exit face of the crystal. The beam size along the y axis is ~ 55 μm, slightly narrower than the 58 μm initial beam size. The right column of Fig. 4(a) shows the intensity profile at a fixed x position. Analogous results for the other input beam are shown in Fig. 4(b). When both input beams are present, we obtain a STS with no transverse velocity component [Fig. 4(c)]. In all three cases, we observe that the harmonic fields are mutually trapped with the fundamental fields, as expected theoretically. At the exit face of the BBO crystal, the temporal and spatial widths of the STS are very similar to the input values. The temporal profile of the noncollinear STS is shown in Fig. 4(d). The secondary intensity maxima observed 100 and 150 μm from the primary peak in Fig. 4(c) are reproducible. We believe that this nonsoliton radiation appears because the spatial profile of the input beams (which are selected from another beam by apertures) is not very close to the soliton solution.

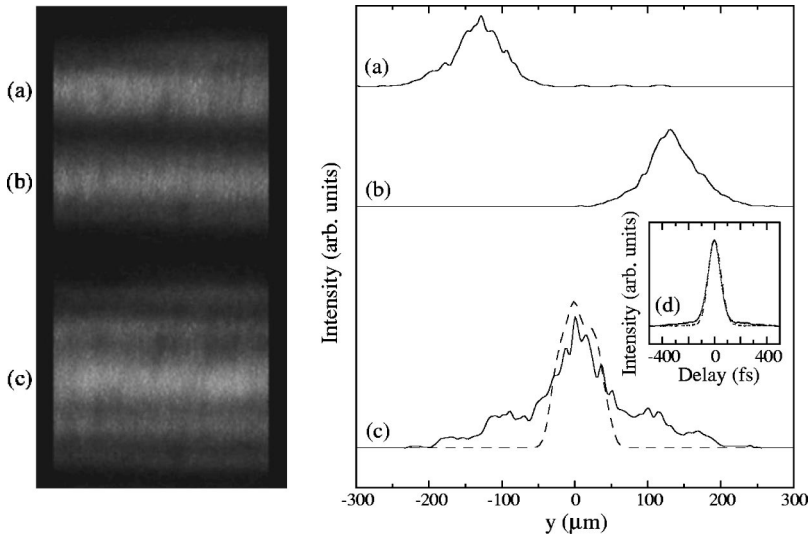

FIG. 4. Experimental spatial and temporal profiles of the output STS under different input conditions: (a) left input field E_L only, (b) right input field E_R only, and (c) E_L and E_R together. The left column contains the images of STS at the exit face, while the plots in the right column are obtained by cuts along a fixed x position. (d) shows the autocorrelation of the output STS in (c). The dashed lines are the profiles of the input pulses.

We also performed a series of control experiments. When the input intensity is reduced below 5 GW/cm^2 or the phase-mismatch is increased in magnitude to over 80π, the nonlinear phase shift produced by the cascade process is inadequate for STS formation. For intensities below 3 GW/cm^2 and $\Delta kL > 150\pi$, we observe approximately linear dispersive and diffractive propagation: the pulse duration and beam diameter at the exit face are each ~ 3 times broader than those of the initial pulse. For fixed phase mismatch, the threshold intensity for production of the noncollinear STS is somewhat below that for either beam alone to become an STS. If we increase the intensity to produce individual STS with E_L and E_R, they pass through each other without fusing. With the intensity and phase mismatch optimized for noncollinear STS generation but with the angle between the beams increased to 1.2°, the two input pulses cross each other and form individual STS. With the increase in collision velocity, the attractive force between the two beams is evidently not strong enough to merge them. All of these observations agree with numerical simulations.

If a detector is placed at the bisector of the input beams (Fig. 1), an all-optical AND-gate based on STS can be realized. An obvious advantage of such a device is its high contrast ratio, which is a consequence of the fact that every possible output is a well-defined STS propagating along a unique direction. In contrast to the interactions of quadratic solitons [13], the process we describe has the benefit of being insensitive to the phases of the input pulses. Numerical simulations confirm that phase differences between the input pulses as large as $\pi/2$ do not disrupt the merging process.

A final point is that this work may demonstrate a route to experimental studies of the internal structure of STS. Solitary waves in nonintegrable systems theoretically may have internal eigenmodes [9,14]. Such modes may lead to qualitatively new features in soliton propagation, such as long-lived oscillations of the soliton amplitude. Numerical solutions of noncollinear STS generation at higher initial intensity exhibit much stronger oscillation of the pulse duration and beam size. Future work will address this issue.

In conclusion, we have demonstrated a noncollinear geometry for the generation of 2D STS, based on a type-I interaction in quadratic media. This process can be used to perform the logical AND operation in an ultrafast, all-optical device. It will be interesting to try to combine the unique properties of quadratic solitons (stability even in three dimensions) and Bragg gratings [15] (large anomalous GVD without pulse-front titling) as a route toward integrated logic based on spatiotemporal solitons.

This work was supported by the National Science Foundation under Contract No. ECS-9612255, the National Institutes of Health under Contract No. RR10075, and the Cornell Theory Center. The authors thank H. He for stimulating discussions and A. Gaeta for the use of a digital camera.

[1] X. Liu, L. J. Qian, and F. W. Wise, Phys. Rev. Lett. **82**, 4631 (1999); X. Liu, K. Beckwitt, and F. W. Wise (unpublished).
[2] Y. Silberberg, Opt. Lett. **15**, 1282 (1990).
[3] R. Macleod, K. Wagner, and S. Blair, Phys. Rev. A **52**, 3254 (1995); S. Blair and K. Wagner, Opt. Quantum Electron. **30**, 697 (1998). An alternate approach to soliton-based computation is described in M. H. Jakubowski, K. Steiglitz, and R. Squier, Phys. Rev. E **58**, 6752 (1998).
[4] Y. Baek, R. Schiek, G. I. Stegeman, I. Baumann, and W. Sohler, Opt. Lett. **22**, 1550 (1997).
[5] B. Costantini, C. De Angelis, A. Barthelemy, B. Bourliaguest, and V. Kermene, Opt. Lett. **23**, 424 (1998).
[6] P. D. Drummond, K. V. Kheruntsyan, and H. He, J. Opt. B: Quantum Semiclassical Opt. **1**, 387 (1999).
[7] L. J. Qian, X. Liu, and F. W. Wise, Opt. Lett. **24**, 166 (1999).
[8] L. Torner, D. Mazilu, and D. Mihalache, Phys. Rev. Lett. **77**, 2455 (1996).
[9] L. Torner, C. R. Menyuk, and G. I. Stegeman, J. Opt. Soc. Am. B **12**, 889 (1995); C. Etrich, U. Peschel, F. Lederer, B. Malomed, and Yu. S. Kivshar, Phys. Rev. E **54**, 4321 (1996).
[10] B. A. Malomed, P. Drummond, H. He, A. Berntson, D. Anderson, and M. Lisak, Phys. Rev. E **56**, 4725 (1997).
[11] O. E. Martinez, Opt. Commun. **59**, 229 (1986).
[12] P. Di Trapani, D. Caironi, G. Valiulis, A. Dubietis, R. Danielius, and A. Piskarskas, Phys. Rev. Lett. **81**, 570 (1998).
[13] D.-M. Baboiu and G. I. Stegeman, J. Opt. Soc. Am. B **14**, 3143 (1997).
[14] Yu. S. Kivshar, D. E. Pelinovsky, T. Cretegny, and M. Peyrard, Phys. Rev. Lett. **80**, 5032 (1998).
[15] B. J. Eggleton, R. E. Slusher, C. M. deSterke, P. A. Krug, and J. E. Sipe, Phys. Rev. Lett. **76**, 1627 (1996); H. He and P. D. Drummond, *ibid.* **78**, 4311 (1997).